ACS OMEGA

Open Access

http://pubs.acs.org/journal/acsodf

Article

Collagenase and Tyrosinase Inhibitory Compounds from Fish Gut Bacteria *Ruegeria atlantica* and *Pseudoalteromonas neustonica*

Jonghwan Kim,[#] Su Jung Hwang,[#] Gyu Sung Lee,[#] Ju Ryeong Lee, Hye In An, Hong Sik Im, Minji Kim, Sang-Seob Lee, Hyo-Jong Lee,[*] and Chung Sub Kim[*]

Cite This: *ACS Omega* 2024, 9, 34259−34267

Read Online

ACCESS | Metrics & More | Article Recommendations | Supporting Information

ABSTRACT: *Ruegeria atlantica* and *Pseudoalteromonas neustonica* are fish gut bacteria that have been isolated from the guts of *Pagrus major* and *Acanthopagrus schlegelii*, respectively. A total of 22 compounds (**1**−**22**) were isolated from these two bacteria; 16 compounds (**1**−**16**) from *R. atalantica* and 6 compounds (**17**−**22**) from *P. neustonica*. Their chemical structures were elucidated by spectroscopic and spectrometric data analysis and chemical synthesis. Compounds **11** and **13** showed strong collagenase inhibitory activity, with 31.91% and 36.43% at 20 μM, respectively, comparable to or surpassing that of the positive control epigallocatechin gallate (EGCG, 34.66%). Also, compounds **11** and **14** exhibited a mild tyrosinase inhibitory effect of 6.73% and 13.68%, respectively. All of the tested compounds displayed no significant antibacterial activity against *Escherichia coli* and *Bacillus subtilis* up to 100 μM. The collagenase- and tyrosinase-inhibitory compound **11**, cyclo(L-Pro-D-Leu), was found to be stable under heat (50 °C) and UV light (254 and 365 nm) for up to 6 days. These results indicate that compound **11** could be developed into a cosmeceutical with antiaging effects.

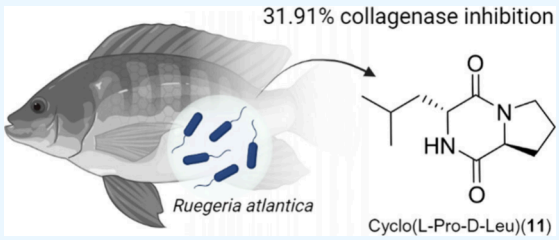

1. INTRODUCTION

Natural products have long served as important sources of new drugs. Out of the 1,881 drugs approved by the FDA between 1981 and 2019, 930 are either natural products themselves or natural product-related drugs, accounting for 49.2%.[1] Given that approximately 98% of metabolites produced by living organisms remain unknown,[2] there are ample opportunities for discovering new drug candidates from various sources, including plants, fungi, and bacteria. In particular, the anticancer compound salinosporamide A, also known as Marizomib, derived from the marine bacterium *Salinispora tropica*, is currently undergoing Phase III clinical trials for the treatment of brain cancer.[3] Beyond their anticancer effects, numerous metabolites from marine bacteria have demonstrated pharmaceutical potential, including antibacterial, antifungal, and antiviral activities,[4] as well as cosmetic applications such as skin whitening and wrinkle improvement.[5]

The enzymes tyrosinase, tyrosinase-related protein-1 and 2 (TRP-1 and 2), collectively known as the tyrosinase gene family, play a crucial role in melanin synthesis.[6] Tyrosinase mediates the transformation of L-tyrosine into 3,4-dihydroxy-L-phenylalanine (L-DOPA) through hydroxylation, followed by the conversion of L-DOPA to L-dopaquinone via oxidation.[7,8] The resultant L-dopaquinone subsequently undergoes a sequence of nonenzymatic processes to ultimately yield eumelanin.[9] Genetically, a high rate of melanin production is primarily associated with the upregulation of the microphthalmia-associated transcription factor (MITF), which controls the transcription of the tyrosinase gene family.[10] Given the indispensable role of tyrosinase in melanin synthesis, various inhibitory compounds targeting tyrosinase have been suggested as potential remedies for skin disorders linked to melanin and/or skin whitening.[11,12] Among these, kojic acid and arbutin have been used in cosmetic applications and have shown robust therapeutic outcomes. Hydroquinone, on the other hand, has been banned as a cosmetic ingredient since 2001 due to its severe side effects, despite its excellent whitening properties.[13−15] Collagen plays a vital role in maintaining the health of human skin as it contributes to its structural integrity, elasticity, firmness, and flexibility. Collagenases are enzymes responsible for breaking down collagen within the skin, leading to the development of wrinkles as we grow older. Thus, substances with the capability to hinder the activity of these enzymes hold promise in retarding the formation of wrinkles and, consequently, the aging process.[16−18]

Ruegeria atlantica KEMB 21431 and *Pseudoalteromonas neustonica* KEMB 21433 were isolated from the guts of *Pagrus major* and *Acanthopagrus schlegelii*, respectively. No research

Received: November 30, 2023
Revised: July 9, 2024
Accepted: July 11, 2024
Published: July 29, 2024

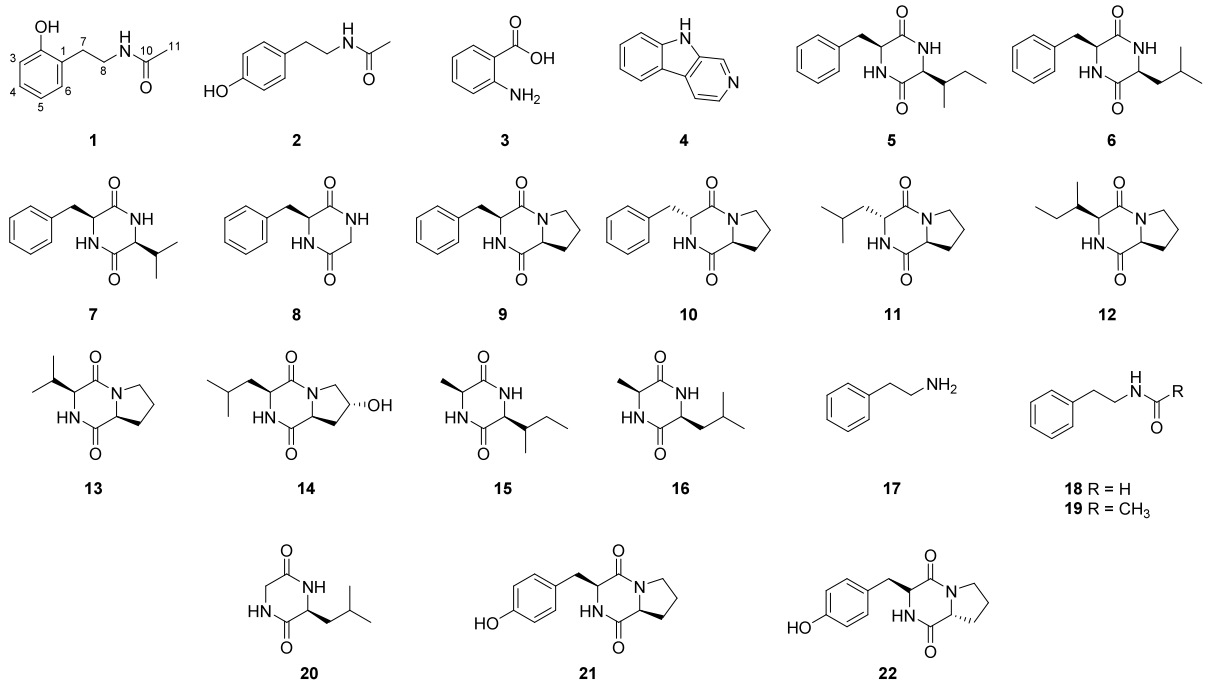

Figure 1. Chemical structures of compounds isolated from *R. atlantica* (**1**−**16**) and *P. neustonica* (**17**−**22**).

has been undertaken on the metabolites produced by *R. atlantica* and *P. neustonica* since their first isolation in 1992 and 2016, respectively.[19−21] Therefore, we conducted an investigation on their metabolites. In this study, we discuss the isolation of 22 compounds (Figure 1) from these two marine bacterial culture extracts and the identification of their chemical structures using conventional NMR and MS data analysis as well as chemical synthesis. Furthermore, we investigated the collagenase- and tyrosinase-inhibitory activities of these compounds to propose them as potential functional cosmetic ingredients, along with antibacterial tests.

2. RESULTS AND DISCUSSION

2.1. Isolation and Structure Elucidation of 1−22.

Compound **1** was isolated from *R. atlantica* KEMB 21431 and its molecular formula was established as $C_{10}H_{13}NO_2$, displaying a positive-ion peak $[M + H]^+$ at *m*/*z* 180.1 (calcd for $C_{10}H_{14}NO_2^+$, 180.1). The ^{1}H NMR spectrum of **1** displayed the presence of a 1,2-disubtituted benzene ring [δ_H 7.14 (1H, td, *J* = 7.71, 1.72 Hz, H-4), 7.04 (1H, dd, *J* = 7.45, 1.70 Hz, H-6), 6.89 (1H, dd, *J* = 8.07, 1.19 Hz, H-3) and 6.82 (1H, td, *J* = 7.35, 1.20 Hz, H-5)], two methylenes [δ_H 3.37 (2H, m, H-8) and 2.86 (2H, m, H-7)] and a methyl group [δ_H 1.90 (3H, s, H-11)]. The ^{13}C NMR spectrum of **1** showed ten carbon signals, including a carbonyl carbon [δ_C 171.6 (C-10)], six aromatic carbons [δ_C 155.4 (C-2), 130.4 (C-6), 128.4 (C-4), 124.5 (C-1), 120.2 (C-5) and 116.5 (C-3)], two methylene carbons [δ_C 40.7 (C-8) and 30.7 (C-7)], and a methyl carbon [δ_C 23.2 (C-11)] (Table 1). Further spectroscopic data analysis of two-dimensional (2D) NMR [correlation spectroscopy (COSY), heteronuclear single quantum correlation (HSQC), and heteronuclear multiple bond correlation (HMBC)] showed three partial structures (units **A**−**C**) (Figure 2). The COSY correlations of H-3(δ_H 6.89)/H-4(δ_H 7.14), H-4(δ_H 7.14)/H-5(δ_H 6.82) and H-5(δ_H 6.82)/H-6(δ_H 7.04) and the HMBC correlations of H-4(δ_H 7.14)/C-2(δ_C 155.4), H-5(δ_H 6.82)/C-1(δ_C 124.5) and H-3(δ_H 6.89)/C-1(δ_C 124.5) supported the presence of the 1,2-disubtituted benzene ring, the unit **A**. The structure of unit **B**, the ethylamino group, was proposed by the COSY correlations of H-7(δ_H 2.86)/H-8(δ_H 3.37) and the HMBC cross-peaks of H-7(δ_H 2.86)/C-8(δ_C 40.7) and H-8(δ_H 3.37)/C-7(δ_C 30.7). Finally, the acetyl group, unit **C**, was suggested by the HMBC correlation of H-11(δ_H 2.02)/C-10(δ_C 171.6). The linkage of unit **A** and unit **B** was identified based on the HMBC correlations of H-7(δ_H 2.86)/C-2(δ_C 155.4) and C-6(δ_C

Table 1. ^{1}H and ^{13}C NMR Data of Compound 1 in Chloroform-*d*

	12	
Position	δ_H [mult. (*J* in Hz)]	δ_C
1	−	124.5
2	−	155.3
3	6.89, dd (7.7, 1.2)	116.5
4	7.14, td (7.7, 1.7)	128.4
5	6.82, td (7.7, 1.2)	120.2
6	7.04, dd, (7.7, 1.7)	130.4
7	2.86, m, 2H	30.7
8	3.37, m, 2H	40.7
9-NH	5.95, brs	−
10	−	171.6
11	2.02, s, 3H	23.2
2-OH	7.32, s	−

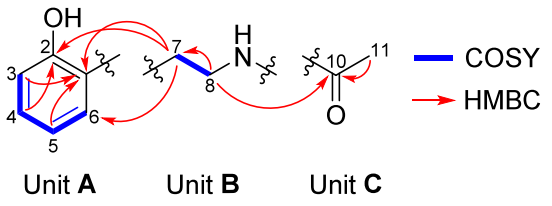

Figure 2. Key COSY (blue bold) and HMBC (red arrow) correlations of **1**.

https://doi.org/10.1021/acsomega.3c09585
ACS Omega 2024, 9, 34259−34267

130.4). The HMBC correlation of H-8(δ_H 3.37)/C-10(δ_C 171.6) showed the connection between unit **B** and unit **C**. Thus, the structure of **1** was defined as *N*-(2-(2-hydroxyphenyl)ethyl)acetamide and further supported by comparing the NMR data of **1** with those previously reported.[22]

Compound **1** has been previously reported only once regarding its isolation from the endophytic fungus *Rosellinia* sp.[22] Our work presents the first isolation of **1** from prokaryotes.

Compounds **2**−**16** and **17**−**22** were isolated from *R. atlantica* KEMB 21431 and *P. neustonica* KEMB 21433, respectively. They were identified by comparing their observed spectroscopic data with those reported in the literatures as *N*-acetyltyramine (**2**),[23] anthranilic acid (**3**),[24] *β*-carboline (**4**),[25] cyclo(L-Phe-L-Ile) (**5**),[26] cyclo(L-Phe-L-Leu) (**6**),[27] cyclo(L-Phe-L-Val) (**7**),[28] cyclo(D-Phe-Gly) (**8**),[29] cyclo(L-Pro-L-Phe) (**9**),[30] cyclo(L-Pro-D-Phe) (**10**),[31] cyclo(L-Pro-D-Leu) (**11**),[31] cyclo(L-Pro-L-Ile) (**12**),[30] cyclo(L-Pro-L-Val) (**13**),[32] cyclo(L-(4-OH)-Pro-L-Leu) (**14**),[33] cyclo(L-Ile-L-Ala) (**15**),[33] cyclo(L-Ala-L-Leu) (**16**),[34] 2-phenylethylamine (**17**),[35] *N*-(2-phenylethyl)formamide (**18**),[36] *N*-(2-phenylethyl)acetamide (**19**),[37] cyclo(Gly-L-Leu) (**20**),[38] cyclo(L-Pro-L-Tyr) (**21**),[39] and cyclo(D-Pro-L-Tyr) (**22**).[39] To the best of our knowledge, this is the first metabolite investigation on *R. atlantica* and *P. neustonica*.

2.2. Biomimetic Synthesis of 18. Based on the characterized structures of **17**−**19**, which share the core structure of 2-phenethylamine (**17**), we assumed that **18** and **19** could be biosynthesized by formylation and acetylation, respectively, from **17**. Moreover, our group recently confirmed that formaldehyde is produced from a bacterial species, *Bacillus licheniformis*.[40] To test this proposal, we performed biomimetic synthesis of **18** from 2-phenethylamine (**17**) and formaldehyde, two potential biosynthetic precursors of **18**. We incubated 2-phenethylamine (**17**) and formaldehyde without bacteria in distilled water at 37 °C for 24 h (Figure 3). As

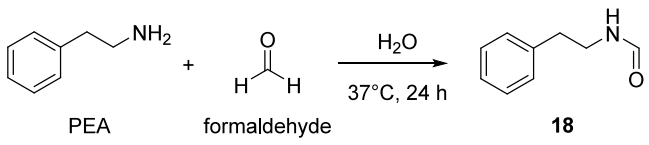

Figure 3. Chemical synthesis of **18** from phenethylamine (PEA) and formaldehyde.

anticipated, compound **18** (0.12 mg, 4.6% w/w) was produced from the reaction mixture. We propose that hemiaminal intermediate would be produced by coupling a phenethylamine and a formaldehyde molecule, which would then oxidize to form **18** (Figure S49).[41] The structure of synthesized **18** was identified to be the same as that of the bacteria-derived metabolite by comparing its ^{1}H NMR data (Figure S37).

2.3. Effect of Compounds 1−22 on Cell Viability. The impact of compounds **1**−**22** on cell viability in mouse B16F10 melanocytes was assessed using the 3-(4,5-dimethyl-thiazol-2-y1)-2,5-diphenyltetrazolium bromide (MTT) assay, as demonstrated in Figure 4. Cell viability of most compounds remained over 90% within the concentration range of 3.125 to 50 μM, except for compound **15**, which displayed approximately 85% cell viability at 50 μM. Based on the results in Figure 4, it can be concluded that these compounds do not exhibit cytotoxicity toward mouse melanocyte cells in the concentration range of 3.125 to 50 μM.

2.4. Effect of Compounds 1−22 on Tyrosinase Family Gene Expression. Considering that microphthalmia-associated transcription factor (MITF) plays a pivotal role in governing pigmentation processes as a key transcription factor,[42] we examined how the compounds impact the expression of MITF and its target genes, including tyrosinase, TRP-1 and 2, using real-time RT-PCR. When B16F10 cells were cotreated with α-melanocyte-stimulating hormone (α-MSH) and 20 μM of the compounds, as shown in Figure 5, compounds **1**−**5**, **8**, **10**−**12**, **14**, **15**, **17**, **19**, **21**, and **22** exhibited more than a 20% reduction in the expression of at least two of the aforementioned target genes. Moreover, compounds **1**−**5**, **10**−**12**, **14**, **15**, **19**, and **22** displayed a substantial decrease of over 40% in the expression of more than one target gene. Among these, compounds **3**, **11**, and **14** exhibited remarkable inhibition by suppressing the expression of more than two target genes at rates exceeding 40% and 60%, respectively.

2.5. Effect of Compounds 3, 11, and 14 on Antityrosinase Activity *In Vitro*. To evaluate the whitening potential of compounds **3**, **11**, and **14**, we measured the activity of tyrosinase, an enzyme involved in melanin production. As a positive control, kojic acid (5-hydroxy-2-hydroxymethyl-1,4-pyrone) was used, which is a well-known whitening agent in cosmetics. The inhibition percentages of these compounds at a concentration of 20 μM are depicted in Figure 6. Compound **14** exhibited a 13.68% inhibition rate of tyrosinase activity, whereas compounds **3** and **11** displayed weaker inhibitory effects compared to compound **14** (1.84% and 6.73%, respectively).

2.6. Effect of Compounds 1−22 on Collagenase Activity. The compounds were examined for their inhibitory effects on collagenase, and the results are illustrated in Figure 7. As a positive control, EGCG exhibited about 34.66% inhibition of collagenase activity. Notably, at a concentration of 20 μM, compounds **11** and **13** demonstrated inhibition rates of 31.91% and 36.43%, respectively, which are comparable to that of EGCG. Furthermore, compounds **2**, **3**, **4**, **5**, **7**, **8**, **9**, **10**, **12**, **14**, **15**, and **18** displayed collagenase inhibitory rates exceeding 15%, suggesting that these compounds have the potential to produce antiwrinkle effects through the inhibition of collagenase activity.

2.7. Antibacterial Activity of 1−22. The isolated compounds **1**−**22** were evaluated for their antibacterial activities against two representative Gram-positive and Gram-negative bacteria, *Bacillus subtilis* and *Escherichia coli*. However, no antibacterial activity was observed in the range 0.39−100 μM of these compounds.

2.8. Stability Test of 11 against Light and Heat. To survey cosmeceutical usage of collagenase- and tyrosinase-inhibitory compound **11**, a stability test against light (UV 254 and 365 nm) and heat (50 °C) was carried out using a 700 MHz NMR spectrometer. The stability percentages were determined by comparing the calculated integration ratio of the H-6 peak to the solvent peak of initial NMR spectrum. As a result, after 6 days, compound **11** showed 96.30−99.53% stability in UV 254 and 365 nm light in DMSO-d_6 and methanol-d_4 solvents and 96.62−97.63% stability at 50 °C in the same condition as described above (Table 2, Figures S46−S63).

https://doi.org/10.1021/acsomega.3c09585
ACS Omega 2024, 9, 34259−34267

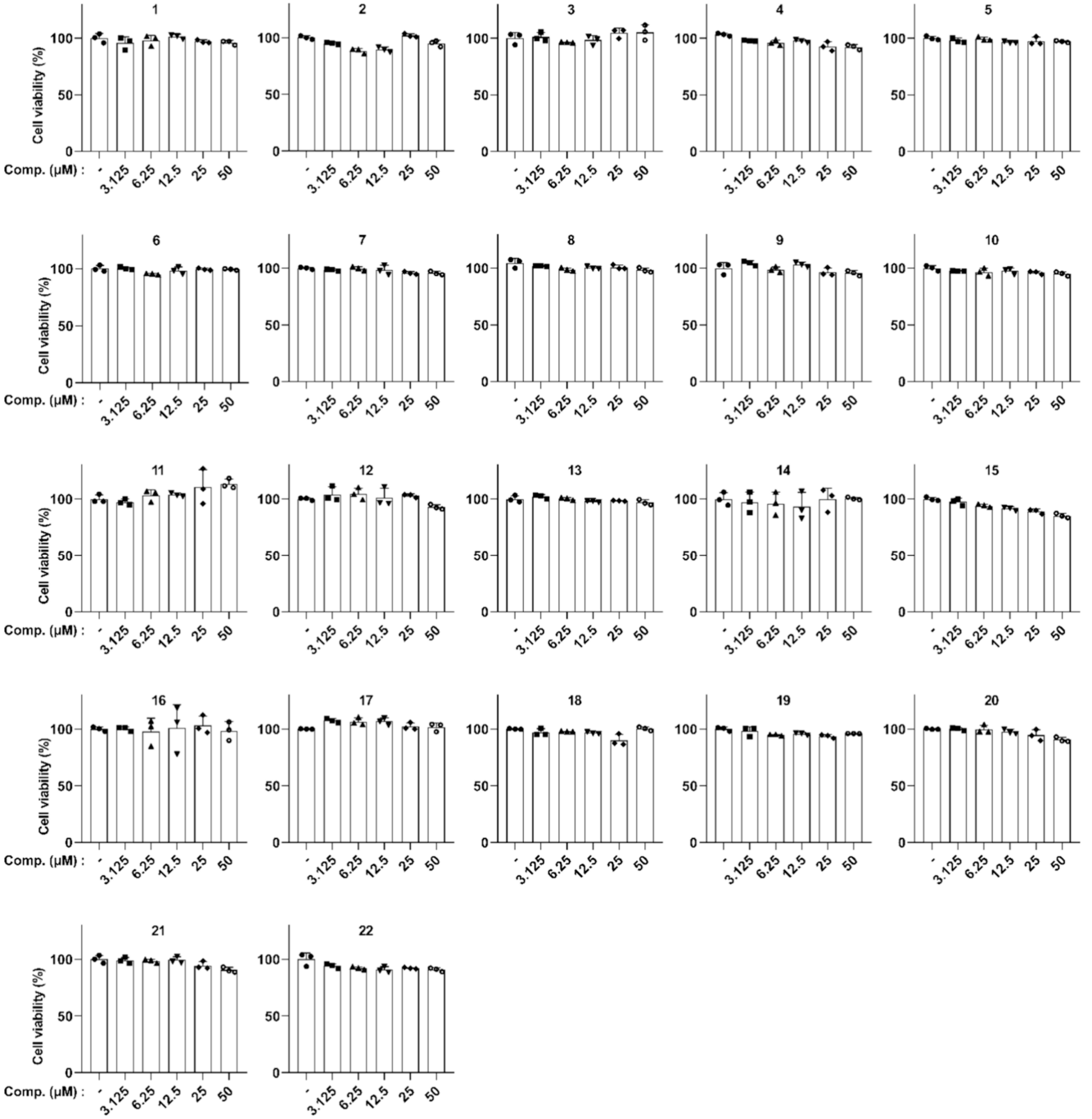

Figure 4. Assessment of *in vitro* toxicity of compounds **1**−**22**. Toxicity studies were performed in B16F10 cells. MTT assays were conducted after cultures were treated with the indicated concentrations of each compound for 24 h. All experiments were conducted at least three times. The bars represent the mean ± SD.

3. EXPERIMENTAL SECTION

3.1. General Experimental Procedures. Nuclear magnetic resonance (NMR) spectra were recorded with a Bruker AVANCE III 700 NMR spectrometer with chemical shifts given in parts per million (δ) (Bruker, Karlsruhe, Germany). All HRESIMS spectra were obtained using an Agilent G6545B quadrupole time-of-flight mass spectrometer (Agilent Technologies) coupled to an Agilent 1260 Infinity II series furnished 6545 LC-Q-TOF mass spectrometer (Agilent Technologies) with an Agilent EclipsePlus C_{18} column (50 × 2.1 mm i.d., 1.8 μm; flow rate: 0.3 mL/min). The LC-MS analysis was performed on an Agilent 1260 series HPLC system with a diode array detector and a 6130 Series ESI mass spectrometer equipped with an analytical Kinetex C_{18} 100 Å column (250 mm × 4.6 mm inner diameter, 5 μm; flow rate: 0.7 mL/min). Semipreparative HPLC was conducted using an Agilent 1260 pump, which was equipped with a Luna C_{18} 100 Å column (250 mm × 10 mm i.d., 5 μm; flow rate: 4.0 mL/min) and a Luna 5 μ Phenyl-Hexyl column (250 mm × 10 mm i.d., 5 μm; flow rate: 4.0 mL/min).

3.2. Bacterial Sources. The marine bacteria *R. atlantica* KEMB 21431 *and P. neustonica* KEMB 21433 were isolated from gut of fish, *P. major* and *A. schlegelii*, respectively. These

https://doi.org/10.1021/acsomega.3c09585
ACS Omega 2024, 9, 34259−34267

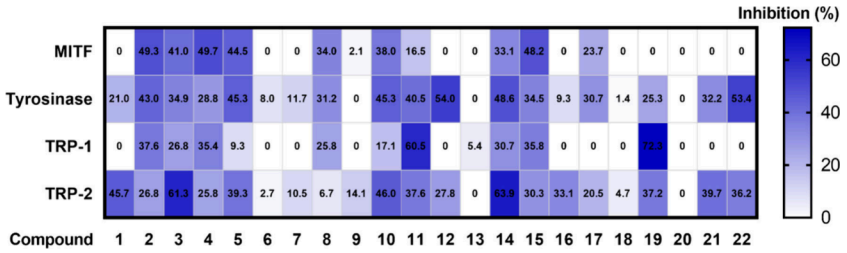

Figure 5. Inhibition of melanogenesis-related gene expression by compounds **1**−**22** in B16F10 melanoma cells. Cells treated with α-MSH alone were used as the control group. Inhibition rate (%) was measured compared to the mRNA level of the control group. All experiments were conducted at least three times.

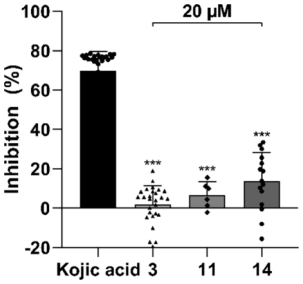

Figure 6. Inhibitory effects of compounds **3**, **11**, and **14** on tyrosinase activity. The results are presented as meta-analysis. Statistical significance was determined using one-way ANOVA followed by a multiple comparisons test. Significance levels are denoted as ***p < 0.001.

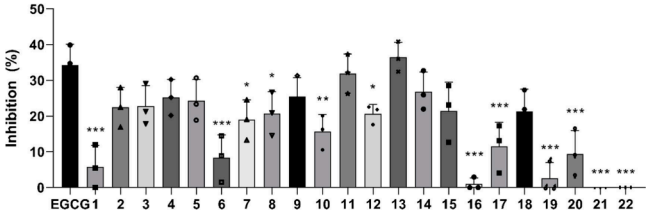

Figure 7. Anticollagenase activity of compounds **1**−**22**. All experiments were conducted at least three times. The bars represent the mean ± SD; *p < 0.05, **p < 0.01, and ***p < 0.001, as determined by one-way ANOVA followed by multiple comparisons test.

Table 2. Stability Test Results of Compound 11

light/heat	Solvent	Duration (day)	Stability (%)
UV 254 nm	DMSO-d_6	3	99.70
		6	99.53
	methanol-d_4	3	96.40
		6	96.30
UV 365 nm	DMSO-d_6	3	99.11
		6	99.08
	methanol-d_4	3	99.84
		6	97.35
50 °C	DMSO-d_6	3	99.32
		6	97.63
	methanol-d_4	3	98.71
		6	96.62

two bacterial strains were provided by the Korea Environmental Microorganisms Bank (KEMB) in Sungkyunkwan University, Korea. *Bacillus subtilis* HB1000 was obtained from Deepika Awasthi (Lawrence Berkeley National Laboratory, University California Berkeley, CA, USA). *Escherichia coli* MG1655 was provided from Dr. Wonsik Lee (Sungkyunkwan University, Suwon, Korea). The frozen stocks of the bacteria used in this study were deposited in the −80 °C freezer of the School of Pharmacy, Sungkyunkwan University, Suwon, Korea.

3.3. Cultivation, Extraction, and Isolation. The strain *R. atlantica* KEMB 21431 was cultured in nine 5 mL tubes with marine broth (MB) media at 30 °C and 250 rpm for 1 day. Subsequently, the cultures were used to inoculate nine 2 L Erlenmeyer flasks containing 9 L of MB media and incubated at 30 °C, 250 rpm. After 5 days, the entire culture was extracted twice with 9 L of ethyl acetate, and the ethyl acetate-soluble layer was concentrated under reduced pressure to yield a crude extract. This procedure was repeated six times to obtain 2.6 g of dried extract.

The dried extract of *R. atlantica* KEMB 21431 was fractionated using a semipreparative HPLC system [Phenomenex, Luna 10 μm $C_{18}(2)$ 250 mm × 10 mm i.d.] with a gradient elution ranging from 10% to 100% aqueous MeCN containing 0.01% trifluoroacetic acid (TFA) over 30 min (flow rate: 4 mL/min), resulting in the collection of 30 fractions, R1 to R30. Compound **13** (t_R 9.3 min, 0.17 mg) was isolated from the fraction R3 through HPLC purification [Phenomenex, Luna 10 μm $C_{18}(2)$ 250 mm × 10 mm i.d.]. The gradient system was optimized as follows: 0−7 min 1% MeCN with 0.01% TFA; 7−13 min 1−3.5% MeCN with 0.01% TFA; 13−18 min 3.5% MeCN with 0.01% TFA; 18−35 min 3.5−15% MeCN with 0.01% TFA (flow rate 4 mL/min for 35 min). Fraction R8 was separated using HPLC system [Phenomenex, Luna 10 μm $C_{18}(2)$ 250 mm × 10 mm i.d.]. A gradient elution method was applied, starting with 8% aqueous MeCN with 0.01% TFA (flow rate 4 mL/min for 5 min), followed by a gradient from 8−11.5% aqueous MeCN with 0.01% TFA (flow rate 4 mL/min for 30 min). This process resulted in the collection of three subfractions: R8-1 (t_R 14−16 min), R8-2 (t_R 16.2−18.2 min) and R8-3 (t_R 19.2−20.7 min). Three subfractions were further purified by an HPLC system [Phenomenex, Luna Phenyl-hexyl, 10 μm, 250 mm × 10 mm i.d.]. A gradient elution method was applied, starting with 8% aqueous MeCN with 0.01% TFA (flow rate 4 mL/min for 5 min), followed by a gradient from 8−11.5% aqueous MeCN with 0.01% TFA (flow rate 4 mL/min for 30 min). From subfraction R8-1, compound **8** (t_R 17.4 min, 1.83 mg) was isolated. From subfraction R8-2, compounds **2** (t_R 15.2 min, 1.99 mg), **14** (t_R 18 min, 1.17 mg) and **15** (t_R 18.9 min, 1.10 mg) were isolated. From subfraction R8-3, compound **16** (t_R 21.9 min, 0.15 mg) was isolated. Fraction R10 was separated by an HPLC system [Phenomenex, Luna 10 μm $C_{18}(2)$ 250 mm × 10 mm i.d.] using a gradient with 15−15.5% aqueous MeCN with 0.01% TFA (flow rate 4 mL/min for 30 min) to give compounds **4** (t_R 17.2 min, 0.19 mg), **9** (t_R 16.9 min, 6.52

https://doi.org/10.1021/acsomega.3c09585
ACS Omega 2024, 9, 34259−34267

mg), **11** (t_R 14.9 min. 6.44 mg), **12** (t_R 13.1 min, 6.74 mg) and subfraction R10-1(t_R 15.4−16.2 min). Subfraction R10-1 was further purified using an HPLC system [Phenomenex, Luna 10 μm C_{18}(2) 250 mm × 10 mm i.d.]. A gradient elution method was applied, starting with 8% aqueous MeCN with 0.01% TFA (flow rate 4 mL/min for 5 min), followed by a gradient from 8−11.5% aqueous MeCN with 0.01% TFA (flow rate 4 mL/min for 30 min). This purification step resulted in the isolation of compounds **1** (t_R 23.2 min, 0.56 mg) and **10** (t_R 25.4 min, 0.37 mg). Fraction R14 was isolated via HPLC [Phenomenex, Luna 10 μm C_{18}(2) 250 mm × 10 mm i.d.] to afford compounds **3** (t_R 13.8 min, 0.15 mg), **5** (t_R 25.3 min, 0.56 mg), **6** (t_R 24.6 min, 0.17 mg) and **7** (t_R 16.8 min, 0.29 mg). The gradient system used in this process was optimized as follows: 0−15 min 20−22.5% aqueous MeCN with 0.01% TFA; 15−25 min 22.5% aqueous MeCN with 0.01% TFA; 25−35 min 22.5−23% aqueous MeCN with 0.01% TFA (flow rate 4 mL/min for 35 min).

The strain *P. neustonica* KEMB 21433 was cultured in nine 5 mL tubes with MB media at 30 °C and 250 rpm for 1 day. Subsequently, the cultures were used to inoculate nine 2 L Erlenmeyer flasks containing 9 L of MB media and incubated at 30 °C, 250 rpm. After 7 days, the entire culture was extracted twice with 9 L of ethyl acetate, and the ethyl acetate-soluble layer was concentrated under reduced pressure to yield a crude extract. This procedure was repeated four times to obtain 2.7 g of dried extract.

The dried extract of *P. neustonica* KEMB 21433 was fractionated using a semipreparative HPLC system [Phenomenex, Luna 10 μm C_{18}(2) 250 mm × 10 mm i.d.] with a gradient elution ranging from 10% to 100% aqueous MeCN containing 0.01% trifluoroacetic acid (TFA) over 40 min (flow rate: 4 mL/min), resulting in the collection of 40 fractions, P1 to P40. Compounds **17** (t_R 13.7 min, 17.2 mg), **20** (t_R 33.0 min, 1.4 mg), **21** (t_R 25.8 min, 0.2 mg) and **22** (t_R 24.4 min, 0.1 mg) were isolated from the fractions P7 and P8 using semiprep HPLC [Phenomenex, Luna 10 μm C_{18}(2) 250 mm × 10 mm i.d.] with a gradient system of 5−6% MeCN with 0.01% TFA (flow rate 4 mL/min for 45 min). Fraction P13 was purified by semiprep HPLC [Phenomenex, Luna Phenylhexyl, 10 μm, 250 mm × 10 mm i.d.] with a gradient system of 15−18% MeCN with 0.01% TFA (flow rate 4 mL/min for 50 min) to afford compounds **18** (t_R 31.5 min, 0.7 mg) and **19** (t_R 33.8 min, 2.3 mg).

3.4. Biomimetic Synthesis of 18. Phenylethylamine (10 mM, Sigma-Aldrich) and formaldehyde (20 mM, Chemone) were reacted in deionized water (20 mL) at 37 °C for 24 h. It was dried with an evaporator and resuspended in 1 mL of methanol to perform LC-MS analysis. Formation of synthetic **18** was confirmed by LC-MS analysis using EICs of corresponding m/z values of natural **18**. Finally, it was purified by semipreparative HPLC [Phenomenex, Luna 10 μm C_{18}(2) 250 mm × 10 mm i.d.], and the ^{1}H NMR of the synthetic **18** was compared with that of natural **18**.

3.5. Cell Viability Assay. Cell viability of B16F10 mouse melanocytes was assessed using an MTT colorimetric assay (Sigma Chemical Co., St. Louis, MO, USA). These cells were cultured in Dulbecco's Modified Eagle's Medium (DMEM; Invitrogen-Gibco BRL, Gaithersberg, MD) at 37 °C in a 5% CO_2 atmosphere. For the *in vitro* cell viability assay, we followed a previously documented procedure.[43] In brief, 5 × 10^3 cells were exposed to varying concentrations of compounds ranging from 3.125 to 50 μM. These cells were allowed to grow to confluence in a 96-well plate over a 24-h period. After the treatment, the supernatants were removed, and a 100 μL aliquot of a 0.5 mg/mL MTT solution was added to each well. The plate was then incubated for 3 h, allowing formazan crystals to precipitate. Subsequently, these crystals were dissolved in DMSO (Sigma Chemical Co., St. Louis, MO, USA). Cell viability was determined by measuring the absorbance at 570 nm using the Tecan Sunrise microplate reader (Tecan Group Ltd., Switzerland).

3.6. RNA Isolation and Real-Time Reverse Transcription-Polymerase Chain Reaction (RT-PCR). Cellular total RNA was extracted, and real-time RT-PCR was carried out according to the previously reported method[43] utilizing the following primer sequences. PCR primers were ordered from Bioneer (Daejeon, Korea): forward β-Actin 5′-AGAGGGAAATCGTGCGTGAC-3′ and reverse β-Actin 5′-GGCCGTCAGGCAGCTCATAG-3′; forward MITF 5′-ATCCCATCCACCGGTCTCTG-3′ and reverse MITF 5′-CCGTCCGTGAGATCCAGAGT-3′; forward tyrosinase 5′-CTCTGGGCTTAGCAGTAGGC-3′ and reverse tyrosinase 5′- GCAAGCTGTGGTAGTCGTCT-3′; forward TRP-1 5′-CAGTGCAGCGTCTTCCTGAG-3′ and reverse TRP-1 5′-TTCCCGTGGGAGCACTGTAA-3′; forward TRP-2 5′-TTCTGCTGGGTTGTCTGGG-3′ and reverse TRP-2 5′-CACAGATGTTGGTTGCCTCG-3′.

3.7. Tyrosinase Inhibition Assay. Tyrosinase inhibitory assay was performed in 96-well plate using enzyme solution, which was prepared by the reconstitution of 4.4 U/μL mushroom tyrosinase (Sigma, St. Louis, MO, USA) in 50 mM potassium phosphate buffer (pH 6.5).[44] A mixture was prepared to achieve the desired final concentrations by combining the following: either 20 μM kojic acid or 1.4 mM kojic acid with L-tyrosine solution, which was then diluted with 50 mM sodium phosphate buffer. The volume of the buffer was adjusted to ensure that the final concentration of L-tyrosine in the reaction mixture was 1.5 mM. Then, 10 μL of mushroom tyrosinase was added, and the enzyme reaction was allowed to proceed for 30 min at 37 °C. After incubation, the amount of dopachrome formed in the reaction mixture was determined by measuring the absorbance at 450 nm.

3.8. Collagenase Inhibition Assay. In the experiment, a fixed weight of 1 mg of Azo dye-impregnated collagen was placed in test tubes. Subsequently, 250 μL of phosphate-buffered saline, along with 200 μL of compounds at a concentration of 20 μM (or EGCG at 2.19 mM as a positive control), and 50 μL of collagenase at a concentration of 200 units/mL were added. After incubating the mixture for 1 h at 43 °C, the test tubes were centrifuged at 3000 rpm for 10 min. The resulting supernatant from each test tube was then transferred to individual 96-well plates, and the absorbance of each supernatant was measured at 540 nm.

3.9. Antibacterial Test. The antibacterial test was performed similarly to our previous research.[45] The two bacterial strains, *E. coli* and *B. subtilis*, were individually streaked on LB agar and incubated for 2 days at 37 °C. A single colony was collected from each LB agar plate and used to inoculate 5 mL of LB broth in a 14 mL polypropylene tube. It was incubated overnight in a shaking incubator at 37 °C, 250 rpm. Then, the OD_{600} value of the bacterial culture was adjusted to 0.001. 196 μL of fresh LB medium and 4 μL of each compound stock solution (10 mM) dissolved in DMSO were added to the first column of a 96-well plate. Using a multichannel pipet, the solution was serially diluted from the

https://doi.org/10.1021/acsomega.3c09585
ACS Omega 2024, 9, 34259−34267

second to the last column of the 96-well plate. Then, 100 μL of the bacterial culture mentioned above (OD_{600} = 0.001) were added to each well. Each experiment was performed three times. The plate was incubated at 37 °C in a standing incubator overnight, and the minimum inhibitory concentration (MIC) value of each compound was obtained from the well where the bacteria were not alive, as determined visually.

3.10. Stability Test. Compound **11** was divided into 6 samples (each 0.3 mg). Half of the samples were dissolved in methanol-d_4, and the others were dissolved in DMSO-d_6. Each sample in methanol-d_4 or DMSO-d_6 was exposed to UV light at 254 or 365 nm or 50 °C for 6 days, respectively. The UV irradiation system was placed in a light-blocking enclosure, with UV light at either 254 or 365 nm as the sole light source. The UV lamp (Spectroline ENF-260C/FE) was used for the UV light source, and the drying oven (Daewon science DS-520S) was used to keep the temperature at 50 °C. ^{1}H NMR spectra of the samples were obtained at days 0, 3, and 6. In various conditions, the maintenance of compound **11** was assessed by measuring the area ratio of the H-6 peak to the solvent peak in the NMR spectrum (rounded to four decimal places). Subsequently, this measurement was utilized to determine the percentage of stability by comparing it with the initial calculated value.

4. CONCLUSIONS

To find skin antiaging metabolites from marine bacteria, we isolated and structurally characterized 22 compounds (**1**−**22**) from the two fish gut-derived bacteria, *R. atlantica* KEMB 21431 and *P. neustonica* KEMB 21433. We further investigated the inhibitory effects of the isolated compounds on enzymes associated with wrinkle formation. Elevated activity of skin enzymes, such as collagenase, can lead to degradation of the extracellular matrix. Collagen breakdown is a major factor in the loss of skin elasticity and reduced skin thickness, which are primary contributors to skin aging and wrinkle formation.[46] Our findings indicate that the compounds **11** and **13** effectively inhibit collagenase activity, the enzyme responsible for collagen degradation, by showing an inhibition rate of more than 30%, without causing any cytotoxic effects. Therefore, these compounds may be considered safe for applications on human skin. In addition, compounds **3**, **11**, and **14** showed significant skin brightening properties. Hyperpigmentation, a contributing factor to human skin aging, results from a combination of internal and external factors, including hormonal shifts, exposure to UV radiation, medications, and contact with various chemicals.[47] Melanin production is a biochemical process that occurs within melanocytes with the enzyme tyrosinase playing a pivotal role in regulating this process. Tyrosinase is essential in two critical stages of melanin synthesis: the conversion of tyrosine to L-DOPA and the subsequent oxidation of L-DOPA to L-dopaquinone.[47] Our findings suggest that these compounds effectively diminish tyrosinase activity, indicating their potential to alleviate hyperpigmentation in human skin.

■ ASSOCIATED CONTENT

Supporting Information

The Supporting Information is available free of charge at https://pubs.acs.org/doi/10.1021/acsomega.3c09585.

Tables S1−S15: ^{1}H NMR data of **2**−**22**. Table S16: Stability results of **11**. Figures S1−S45: UV−vis, MS, and NMR spectra of **1**−**22**. Figures S46−S63: ^{1}H NMR spectra of **11** for stability test. (PDF)

■ AUTHOR INFORMATION

Corresponding Authors

Hyo-Jong Lee − *School of Pharmacy, Sungkyunkwan University, Suwon 16419, Republic of Korea*; Email: pharm79@skku.edu

Chung Sub Kim − *Department of Biopharmaceutical Convergence and School of Pharmacy, Sungkyunkwan University, Suwon 16419, Republic of Korea*; orcid.org/0000-0001-9961-4093; Email: chungsub.kim@skku.edu

Authors

Jonghwan Kim − *Department of Biopharmaceutical Convergence, Sungkyunkwan University, Suwon 16419, Republic of Korea*

Su Jung Hwang − *School of Pharmacy, Sungkyunkwan University, Suwon 16419, Republic of Korea*

Gyu Sung Lee − *Department of Biopharmaceutical Convergence, Sungkyunkwan University, Suwon 16419, Republic of Korea*

Ju Ryeong Lee − *Department of Biopharmaceutical Convergence, Sungkyunkwan University, Suwon 16419, Republic of Korea*

Hye In An − *School of Pharmacy, Sungkyunkwan University, Suwon 16419, Republic of Korea*

Hong Sik Im − *College of Biotechnology and Bioengineering, Sungkyunkwan University, Suwon 16419, Republic of Korea*

Minji Kim − *Department of Biopharmaceutical Convergence, Sungkyunkwan University, Suwon 16419, Republic of Korea*

Sang-Seob Lee − *College of Biotechnology and Bioengineering, Sungkyunkwan University, Suwon 16419, Republic of Korea*

Complete contact information is available at: https://pubs.acs.org/10.1021/acsomega.3c09585

Author Contributions

#J.K., S.J.H., and G.S.L. contributed equally to this work.

Author Contributions

J.K. performed the experiments, analyzed the data, and wrote the manuscript; S.J.H., G.S.L., J.R.L, and H.I.A. performed the experiments and analyzed the data; H.S.I. and M.K. analyzed the data; S.-S.L. provided the bacterial strains; H.-J.L. and C.S.K. conceived the study, oversaw experiments, and wrote the manuscript. All authors have read and agreed to the published version of the manuscript.

Funding

This work was supported by the Marine Biotechnology Program funded by the Ministry of Oceans and Fisheries (No. 20220168), by the National Research Foundation of Korea (NRF) grant funded by the Korean government (MSIT) (No. 2021R1C1C1011045, 2022R1A6A1A030-54419), by the Technology development Program (S3303032 and S3111258) funded by the Ministry of SMEs and Startups (MSS, Korea), by the Sungkyunkwan University, and by the BK21 FOUR (Graduate School Innovation) funded by the Ministry of Education (MOE, Korea) and National Research Foundation of Korea (NRF).

Notes

The authors declare no competing financial interest.

https://doi.org/10.1021/acsomega.3c09585
ACS Omega 2024, 9, 34259−34267

■ ACKNOWLEDGMENTS

TOC graphic was created with BioRender.com.

■ REFERENCES

(1) Newman, D. J.; Cragg, G. M. Natural Products as Sources of New Drugs Over the Nearly Four Decades from 01/1981 to 09/2019. *J. Nat. Prod.* **2020**, *83* (3), 770−803.
(2) da Silva, R. R.; Dorrestein, P. C.; Quinn, R. A. Illuminating the Dark Matter in Metabolomics. *Proc. Natl. Acad. Sci. U. S. A.* **2015**, *112* (41), 12549−12550.
(3) Feling, R. H.; Buchanan, G. O.; Mincer, T. J.; Kauffman, C. A.; Jensen, P. R.; Fenical, W. Salinosporamide A: A Highly Cytotoxic Proteasome Inhibitor from a Novel Microbial Source, a Marine Bacterium of the New Genus *Salinospora*. *Angew. Chem., Int. Ed.* **2003**, *42* (3), 355−357.
(4) Santos, J. D.; Vitorino, I.; Reyes, F.; Vicente, F.; Lage, O. M. From Ocean to Medicine: Pharmaceutical Applications of Metabolites from Marine Bacteria. *Antibiotics* **2020**, *9* (8), 455.
(5) Ding, J.; Wu, B.; Chen, L. Application of Marine Microbial Natural Products in Cosmetics. *Front. Microbiol.* **2022**, *13*, No. 892505.
(6) Kobayashi, T.; Urabe, K.; Winder, A.; Jiménez-Cervantes, C.; Imokawa, G.; Brewington, T.; Solano, F.; García-Borrón, J. C.; Hearing, V. J. Tyrosinase Related Protein 1 (TRP1) Functions as a DHICA Oxidase in Melanin Biosynthesis. *EMBO J.* **1994**, *13*, 5818−5825.
(7) Sánchez-Ferrer, Á.; Rodríguez-López, J. N.; García-Cánovas, F.; García-Carmona, F. Tyrosinase: A Comprehensive Review of Its Mechanism. *Biochim. Biophys. Acta-Protein Struct. Mol. Enzym.* **1995**, *1247* (1), 1−11.
(8) Hearing, V. J.; Ekel, T. M.; Montague, P. M.; Nicholson, J. M. Mammalin Tyrosinase. Stoichiometry and Measurement of Reaction Products. *Biochim. Biophys. Acta-Enzym.* **1980**, *611* (2), 251−268.
(9) Hearing, V. J. Determination of Melanin Synthetic Pathways. *J. Invest. Dermatol.* **2011**, *131* (E1), E8.
(10) Bertolotto, C.; Abbe, P.; Hemesath, T. J.; Bille, K.; Fisher, D. E.; Ortonne, J.-P.; Ballotti, R. Microphthalmia Gene Product as a Signal Transducer in cAMP-Induced Differentiation of Melanocytes. *J. Cell Biol.* **1998**, *142*, 827−835.
(11) Solano, F.; Briganti, S.; Picardo, M.; Ghanem, G. Hypopigmenting Agents: An Updated Review on Biological, Chemical and Clinical Aspects. *Pigment cell Res.* **2006**, *19* (6), 550−571.
(12) Casanola-Martin, G.; Le-Thi-Thu, H.; Marrero-Ponce, Y.; Castillo-Garit, J.; Torrens, F.; Rescigno, A.; Abad, C.; Khan, M. Tyrosinase Enzyme: 1. An Overview on a Pharmacological Target. *Curr. Top. Med. Chem.* **2014**, *14* (12), 1494−1501.
(13) Westerhof, W.; Kooyers, T. Hydroquinone and Its Analogues in Dermatology − A Potential Health Risk. *J. Cosmet. Dermatol.* **2005**, *4* (2), 55−59.
(14) Nohynek, G. J.; Kirkland, D.; Marzin, D.; Toutain, H.; Leclerc-Ribaud, C.; Jinnai, H. An Assessment of the Genotoxicity and Human Health Risk of Topical Use of Kojic Acid [5-hydroxy-2-(hydroxymethyl)-4H-pyran-4-one]. *Food Chem. Toxicol.* **2004**, *42* (1), 93−105.
(15) Takizawa, T.; Imai, T.; Onose, J.-i.; Ueda, M.; Tamura, T.; Mitsumori, K.; Izumi, K.; Hirose, M. Enhancement of Hepatocarcinogenesis by Kojic Acid in Rat Two-Stage Models After Initiation with *N*-bis(2-hydroxypropyl)nitrosamine or *N*-diethylnitrosamine. *Toxicol. Sci.* **2004**, *81* (1), 43−49.
(16) Madan, K.; Nanda, S. *In-vitro* Evaluation of Antioxidant, Anti-Elastase, Anti-Collagenase, Anti-Hyaluronidase Activities of *Safranal* and Determination of Its Sun Protection Factor in Skin Photoaging. *Bioorg. Chem.* **2018**, *77*, 159−167.
(17) Altyar, A. E.; Ashour, M. L.; Youssef, F. S. *Premna odorata*: Seasonal Metabolic Variation in the Essential Oil Composition of Its Leaf and Verification of Its Anti-Ageing Potential via In Vitro Assays and Molecular Modelling. *Biomolecules* **2020**, *10* (6), 879.
(18) Cruz, A. M.; Gonçalves, M. C.; Marques, M. S.; Veiga, F.; Paiva-Santos, A. C.; Pires, P. C. In Vitro Models for Anti-Aging Efficacy Assessment: A Critical Update in Dermocosmetic Research. *Cosmetics* **2023**, *10* (2), 66.
(19) Hwang, C. Y.; Lee, I.; Hwang, Y. J.; Yoon, S. J.; Lee, W. S.; Cho, B. C. *Pseudoalteromonas neustonica* sp. nov., Isolated from the Sea Surface Microlayer of the Ross Sea (Antarctica), and Emended Description of the Genus *Pseudoalteromonas*. *Int. J. Syst. Evol. Microbiol.* **2016**, *66* (9), 3377−3382.
(20) Rüger, H.-J.; Höfle, M. G. Marine star-shaped-aggregate-forming bacteria: *Agrobacterium atlanticum* sp. nov.; *Agrobacterium meteori* sp. nov.; *Agrobacterium ferrugineum* sp. nov., nom. rev.; *Agrobacterium gelatinovorum* sp. nov., nom. rev.; and *Agrobacterium stellulatum* sp. nov., nom. rev. *Int. J. Syst. Evol. Microbiol.* **1992**, *42* (1), 133−143.
(21) Uchino, Y.; Hirata, A.; Yokota, A.; Sugiyama, J. Reclassification of marine Agrobacterium species: Proposals of *Stappia stellulata* gen. nov., comb. nov., *Stappia aggregata* sp. nov., nom. rev., *Ruegeria atlantica* gen. nov., comb. nov., *Ruegeria gelatinovora* comb. nov., *Ruegeria algicola* comb. nov., and *Ahrensia kieliense* gen. nov., sp. nov., nom. rev. *J. Gen. Appl. Microbiol.* **1998**, *44* (3), 201−210.
(22) Cheng, M.-J.; Wu, M.-D.; Aung, T.; Than, N. N.; Hsieh, S.-Y.; Chen, J.-J. Metabolite from the Endophytic Fungus of *Rosellinia* sp. *Chem. Nat. Compd.* **2021**, *57*, 171−173.
(23) Zhao, P. J.; Li, G. H.; Shen, Y. M. New Chemical Constituents from the Endophyte *Streptomyces* species LR4612 Cultivated on *Maytenus hookeri*. *Chem. Biodivers.* **2006**, *3* (3), 337−342.
(24) Hoang, L.; Joo, G.-J.; Kim, W.-C.; Jeon, S.-Y.; Choi, S.-H.; Kim, J.-W.; Rhee, I.-K.; Hur, J.-M.; Song, K.-S. Growth Inhibitors of Lettuce Seedlings from *Bacillus cereus* EJ-121. *Plant Growth Regul.* **2005**, *47*, 149−154.
(25) Wang, Z.-X.; Xiang, J.-C.; Cheng, Y.; Ma, J.-T.; Wu, Y.-D.; Wu, A.-X. Direct Biomimetic Synthesis of β-Carboline Alkaloids from Two Amino Acids. *J. Org. Chem.* **2018**, *83* (19), 12247−12254.
(26) Stark, T.; Hofmann, T. Structures, Sensory Activity, and Dose/Response Functions of 2,5-Diketopiperazines in Roasted Cocoa Nibs (*Theobroma cacao*). *J. Agric. Food Chem.* **2005**, *53* (18), 7222−7231.
(27) Leyte-Lugo, M.; Richomme, P.; Peña-Rodriguez, L. M. Diketopiperazines from *Alternaria dauci*. *J. Mex. Chem. Soc.* **2020**, *64* (4), 283−290.
(28) Saïd Hassane, C.; Herbette, G.; Garayev, E.; Mabrouki, F.; Clerc, P.; de Voogd, N. J.; Greff, S.; Trougakos, I. P.; Ouazzani, J.; Fouillaud, M. New Metabolites from the Marine Sponge *Scopalina hapalia* Collected in Mayotte Lagoon. *Mar. Drugs* **2022**, *20* (3), 186.
(29) Coursindel, T.; Restouin, A.; Dewynter, G.; Martinez, J.; Collette, Y.; Parrot, I. Stereoselective Ring Contraction of 2, 5-Diketopiperazines: An innovative Approach to the Synthesis of Promising Bioactive 5-membered Scaffolds. *Bioorg. Chem.* **2010**, *38* (5), 210−217.
(30) Park, A. R.; Jeong, S.-I.; Jeon, H. W.; Kim, J.; Kim, N.; Ha, M. T.; Mannaa, M.; Kim, J.; Lee, C. W.; Min, B. S. A Diketopiperazine, *cyclo*-(L-Pro-L-Ile), Derived from *Bacillus thuringiensis* JCK-1233 Controls Pine Wilt Disease by Elicitation of Moderate Hypersensitive Reaction. *Front. Plant Sci.* **2020**, *11*, 1023.
(31) Campbell, J.; Lin, Q.; Geske, G. D.; Blackwell, H. E. New and Unexpected Insights into the Modulation of LuxR-Type Quorum Sensing by Cyclic Dipeptides. *ACS Chem. Biol.* **2009**, *4* (12), 1051−1059.
(32) Jiang, Q.; Wei, N.; Huo, Y.; Kang, X.; Chen, G.; Wen, L. Secondary Metabolites of the Endophytic Fungus *Cladosporium* sp. CYC38. *Chem. Nat. Compd.* **2020**, *56*, 1166−1169.
(33) Furtado, N. A.; Pupo, M. T.; Carvalho, I.; Campo, V. L.; Duarte, M. C. T.; Bastos, J. K. Diketopiperazines Produced by an *Aspergillus fumigatus* Brazilian Strain. *J. Braz. Chem. Soc.* **2005**, *16*, 1448−1453.
(34) Vatèle, J.-M. Prenyl Carbamates: Preparation and Deprotection. *Tetrahedron* **2004**, *60* (19), 4251−4260.
(35) Huang, X. X.; Zhou, C. C.; Li, L. Z.; Li, F. F.; Lou, L. L.; Li, D. M.; Ikejima, T.; Peng, Y.; Song, S. J. The Cytotoxicity of 8-*O*-4'

https://doi.org/10.1021/acsomega.3c09585
ACS Omega 2024, 9, 34259−34267

Neolignans from the Seeds of *Crataegus pinnatifida*. *Bioorg. Med. Chem. Lett.* **2013**, *23* (20), 5599−5604.
(36) Zhou, L.; Lou, L.-L.; Wang, W.; Lin, B.; Chen, J.-N.; Wang, X.-B.; Huang, X.-X.; Song, S.-J. Enantiomeric 8-*O*-4' type Neolignans from Red Raspberry as Potential Inhibitors of *β*-Amyloid Aggregation. *J. Funct. Foods* **2017**, *37*, 322−329.
(37) Kim, T. H.; Ito, H.; Hayashi, K.; Hasegawa, T.; Machiguchi, T.; Yoshida, T. Aromatic Constituents from the Heartwood of *Santalum album* L. *Chem. Pharm. Bull.* **2005**, *53* (6), 641−644.
(38) Nakanishi, T.; Iida, N.; Inatomi, Y.; Murata, H.; Inada, A.; Murata, J.; Lang, F. A.; Iinuma, M.; Tanaka, T. Neolignan and Flavonoid Glycosides in *Juniperus communis* var. *depressa*. *Phytochemistry* **2004**, *65* (2), 207−213.
(39) Cimmino, A.; Bejarano, A.; Masi, M.; Puopolo, G.; Evidente, A. Isolation of 2, 5-diketopiperazines from Lysobacter capsici AZ78 with activity against Rhodococcus fascians. *Nat. Prod. Res.* **2021**, *35* (23), 4969−4977.
(40) Ham, S. L.; Lee, T. H.; Kim, K. J.; Kim, J. H.; Hwang, S. J.; Lee, S. H.; Yu, J. S.; Kim, K. H.; Lee, H.-J.; Lee, W. Discovery and Biosynthesis of Imidazolium Antibiotics from the Probiotic *Bacillus licheniformis*. *J. Nat. Prod.* **2023**, *86* (4), 850−859.
(41) Preedasuriyachai, P.; Kitahara, H.; Chavasiri, W.; Sakurai, H. N-Formylation of Amines Catalyzed by Nanogold under Aerobic Oxidation Conditions with MeOH or Formalin. *Chem. Lett.* **2010**, *39* (11), 1174−1176.
(42) Solano, F.; Briganti, S.; Picardo, M.; Ghanem, G. Hypopigmenting Agents: An Updated Review on Biological, Chemical and Clinical Aspects. *Pigment Cell Melanoma Res.* **2006**, *19* (6), 550−571.
(43) Park, J. J.; Hwang, S. J.; Kang, Y. S.; Jung, J.; Park, S.; Hong, J. E.; Park, Y.; Lee, H.-J. Synthesis of Arbutin-Gold Nanoparticle Complexes and Their Enhanced Performance for Whitening. *Arch. Pharm. Res.* **2019**, *42*, 977−989.
(44) Jiang, R.; Um, S.; Jeong, H.; Seo, J.; Huh, M.; Kim, Y. R.; Moon, K. Anti-Melanogenic Dipeptides from a Cretaceous Jinju Formation Derived from *Micromonospora* sp. *Nat. Prod. Sci.* **2023**, *29* (2), 59−66.
(45) Kim, H. R.; Kim, J.; Yu, J. S.; Lee, B. S.; Kim, K. H.; Kim, C. S. Isolation, Structure Elucidation, Total Synthesis, and Biosynthesis of Dermazolium A, an Antibacterial Imidazolium Metabolite of a Vaginal Bacterium *Dermabacter vaginalis*. *Arch. Pharm. Res.* **2023**, *46* (1), 35−43.
(46) Wang, L.; Oh, J. Y.; Yang, H.-W.; Kim, H. S.; Jeon, Y.-J. Protective Effect of Sulfated Polysaccharides from a Celluclast-Assisted Extract of *Hizikia fusiforme* Against Ultraviolet B-Induced Photoaging In Vitro in Human Keratinocytes and In Vivo in Zebrafish. *Mar. Life Sci. Technol.* **2019**, *1*, 104−111.
(47) Costin, G.-E.; Hearing, V. J. Human Skin Pigmentation: Melanocytes Modulate Skin Color in Response to Stress. *Faseb J.* **2007**, *21* (4), 976−994.

https://doi.org/10.1021/acsomega.3c09585
ACS Omega 2024, 9, 34259−34267